

REPORT DOCUMENTATION PAGE			Form Approved OMB NO. 0704-0188		
<p>The public reporting burden for this collection of information is estimated to average 1 hour per response, including the time for reviewing instructions, searching existing data sources, gathering and maintaining the data needed, and completing and reviewing the collection of information. Send comments regarding this burden estimate or any other aspect of this collection of information, including suggestions for reducing this burden, to Washington Headquarters Services, Directorate for Information Operations and Reports, 1215 Jefferson Davis Highway, Suite 1204, Arlington VA, 22202-4302. Respondents should be aware that notwithstanding any other provision of law, no person shall be subject to any penalty for failing to comply with a collection of information if it does not display a currently valid OMB control number. PLEASE DO NOT RETURN YOUR FORM TO THE ABOVE ADDRESS.</p>					
1. REPORT DATE (DD-MM-YYYY) 31-03-2021		2. REPORT TYPE Final Report		3. DATES COVERED (From - To) 21-Dec-2018 - 20-Dec-2020	
4. TITLE AND SUBTITLE Final Report: Multi-terminal Josephson circuits supporting nontrivial Chern topologies for anyonic qubits			5a. CONTRACT NUMBER W911NF-19-1-0067		
			5b. GRANT NUMBER		
			5c. PROGRAM ELEMENT NUMBER 611102		
6. AUTHORS			5d. PROJECT NUMBER		
			5e. TASK NUMBER		
			5f. WORK UNIT NUMBER		
7. PERFORMING ORGANIZATION NAMES AND ADDRESSES University of Illinois - Urbana - Champaign c/o Office of Sponsored Programs 1901 S. First Street, Suite A Champaign, IL 61820 -7406			8. PERFORMING ORGANIZATION REPORT NUMBER		
9. SPONSORING/MONITORING AGENCY NAME(S) AND ADDRESS (ES) U.S. Army Research Office P.O. Box 12211 Research Triangle Park, NC 27709-2211			10. SPONSOR/MONITOR'S ACRONYM(S) ARO		
			11. SPONSOR/MONITOR'S REPORT NUMBER(S) 73791-EL.3		
12. DISTRIBUTION AVAILABILITY STATEMENT Approved for public release; distribution is unlimited.					
13. SUPPLEMENTARY NOTES The views, opinions and/or findings contained in this report are those of the author(s) and should not be construed as an official Department of the Army position, policy or decision, unless so designated by other documentation.					
14. ABSTRACT					
15. SUBJECT TERMS					
16. SECURITY CLASSIFICATION OF:			17. LIMITATION OF ABSTRACT UU	15. NUMBER OF PAGES	19a. NAME OF RESPONSIBLE PERSON Alexey Bezryadin
a. REPORT UU	b. ABSTRACT UU	c. THIS PAGE UU			19b. TELEPHONE NUMBER +12-173-3395

# RPPR Final Report

## as of 19-Apr-2021

Agency Code: 21XD

Proposal Number: 73791EL

Agreement Number: W911NF-19-1-0067

### INVESTIGATOR(S):

**Name:** Ph.D. Alexey Bezryadin  
**Email:** bezryadi@illinois.edu  
**Phone Number:** +12173339580  
**Principal:** Y

**Name:** Ph.D. James N Eckstein  
**Email:** eckstein@illinois.edu  
**Phone Number:** +12172447709  
**Principal:** N

Organization: **University of Illinois - Urbana - Champaign**

Address: c/o Office of Sponsored Programs, Champaign, IL 618207406

Country: USA

DUNS Number: 041544081

EIN: 376000511

**Report Date:** 20-Mar-2021

Date Received: 31-Mar-2021

**Final Report** for Period Beginning 21-Dec-2018 and Ending 20-Dec-2020

**Title:** Multi-terminal Josephson circuits supporting nontrivial Chern topologies for anyonic qubits

**Begin Performance Period:** 21-Dec-2018

**End Performance Period:** 20-Dec-2020

**Report Term:** 0-Other

Submitted By: Ph.D. Alexey Bezryadin

Email: bezryadi@illinois.edu

Phone: (+12) 173-339580

**Distribution Statement:** 1-Approved for public release; distribution is unlimited.

**STEM Degrees:** 1

**STEM Participants:** 4

**Major Goals:** Topological superconductors are among the most unconventional states of matter, wherein exotic p-wave pairing and time-reversal symmetry can foster supersymmetry and zero-energy excitations called Majorana bound states. Although potential applications of theoretically proposed topologically protected quantum computers are numerous, the basic demonstration of non-Abelian behavior has not been achieved yet. Thus, our major goal is to design fabricate and test suitable electronic devices which can unambiguously demonstrate topological protection and non-Abelian behavior.

Among many obstacles, the materials issues are still of great importance: Many of the synthesized topological insulator materials exhibit bulk conductivity, while, in theory, only the surface is supposed to be conducting, while the bulk conductivity should be zero. Thus, an important goal of this project is to discover, develop, synthesize, and test novel topological systems approaching the ideal case in which the current is carried predominantly by the topological states. Another goal is to characterize these materials using available powerful techniques, providing access to the electronic spectrum structure, such as angle-resolved photoemission spectroscopy (ARPES).

As the material issues get improved, we target implementations of novel hybrid devices and structure involving the top-quality topological insulators interfaced with superconducting Nb films. In such systems, superconducting electrons penetrates into the topological insulator, due to the proximity effect. The induced superconductivity is expected to acquire topological properties of the host topological insulator.

The main plan is to fabricate multiterminal devices in which non-Abelian Majorana particles are predicted theoretically. The devices and systems should allow flexibility and control over the phase of the induced, complex-function, superconducting order parameter. The guiding principle is that the Majorana states are expected in the segments of Josephson junctions at which the phase difference equals  $\pi$ . If such condition is satisfied, the energy of the quasiparticles approaches zero, and, due to the underlying topological properties, the localized quasiparticles should become the desired non-Abelian Majorana states.

The key feature of the Majorana zero modes is that they have a ground state degeneracy characterized by the so-called "parity". This degeneracy, if discovered, can be used for storing and processing quantum information in a topologically protected manner. Yet, they parity has not been observed in any experiment yet. Another fundamental property of the Majorana zero modes is called braiding. The physical meaning of this property is that if two Majorana localized modes are moved around each other then the ground state should change its parity. This way one hopes to be able to process quantum information in the future topologically protected quantum computers.

# RPPR Final Report

## as of 19-Apr-2021

A long-term goal of this project is to design systems where such fundamental properties of the Majorana states could be demonstrated.

Practically, our approach is to focus on arrays with multiple electrodes and multiple superconducting islands, coupled to high quality epitaxial topological insulator films. In such systems phase differences of the complex superconducting order parameter can be controlled by applying external magnetic fields. Thus, it should be possible to induce Majorana zero modes, which are expected to occur in Josephson vortices. The parity effect should be detectable as fluctuations of the net supercurrent in the system or fluctuations of the critical current/kinetic inductance. Thus, the braiding phenomenon can probably be tested by moving vortices in and out the array, assuming that some vortices will experience an entanglement of their paths. Precise control of the vortex position can also be achieved if calibrated current pulses are applied. Such braiding events should cause parity changes and should be detectable in transport or the kinetic inductance measurements.

**Accomplishments:** One major result of this project is the ultrahigh-resolution ARPES mappings of clean, bulk insulating  $(\text{Bi}_{1-x}\text{Sbx})_2\text{Te}_3$  ( $x \sim 0.62$ ) on superconducting Nb substrate as a function of TI film thickness and temperature. This material is extraordinary since it is an intrinsic topological insulator. The Fermi level in this material is tuned to the topological states and it avoids bulk conduction states. The results, combined with the previous studies of the  $\text{Bi}_2\text{Se}_3/\text{Nb}$  interface, reveal the pivotal role of bulk states in transiting superconductivity to the surfaces of TIs-Nb hybrid systems [ ].

This project is motivated by the following considerations. Topological superconductors are among the most unconventional states of matter, wherein exotic p-wave-like pairing and time-reversal symmetry can foster supersymmetry and zero-energy excitations called Majorana bound states. These emergent quasiparticles obey a non-Abelian statistics pertinent to topological quantum computing. Despite some recent progress, robust topological superconducting states remain elusive due to, often small, superconducting gap and low transition temperature in candidate materials. One promising alternative for realizing this state is to couple topological insulators (TIs) to a superconductor (SC) so that p-wave-like pairing is induced into the topological boundary states via the superconducting proximity effect. Thus, the proximity effect is at the focus of this project.

In this project the superconductor of choice, needed to introduce superconductivity in the hybrid systems, is Nb. To circumvent the inherent difficulties in growing TIs on Nb substrates, a novel cleavage-based flip-chip method is employed (Fig.1), which upon cleaving yields the intrinsic TI films of specific thicknesses, even in the ultrathin-film limit, on superconducting bulk Nb films.

Figure 1. Photo and diagram of flip-chip sample structure before cleavage. (g) Similar as in (f) but after cleavage.

Proximity-induced superconducting gaps for slightly n-doped intrinsic topological insulator  $(\text{Bi}_{1-x}\text{Sbx})_2\text{Te}_3$  are quantified and contrasted with those of n-doped  $\text{Bi}_2\text{Se}_3/\text{Nb}$  from prior work conducted in the Eckstein group. Proximity induced is observed and it is found that it is significantly stronger in the  $\text{Bi}_2\text{Se}_3/\text{Nb}$  system. But this system has a much larger concentration of bulk carriers. Thus, an important conclusion is reached that the bulk state, which are also made superconducting due to the proximity effect, play a key role in inducing superconductivity in the top topological layer of the TI.

The series of square arrays and triangular arrays has been produced (Fig.2) and systematic measurements have been performed (Fig.3). Each array is a lattice of superconducting Nb islands placed onto a topological insulator film, such as  $\text{Bi}_2\text{Se}_3$  or  $(\text{Bi}_{1-x}\text{Sbx})_2\text{Te}_3$ . The square arrays exhibit, reproducibly, a series of the critical current maximum, as the magnetic field is swept.

We demonstrate that placing an ordinary superconductor in a direct contact with a topological insulator (TI) enables topological superconductivity due to the proximity effect. Such systems have been predicted to harbor non-Abelian excitations known as Majorana zero modes. We have studied matching fields and the critical currents of square arrays of superconducting Nb islands placed onto topological insulator epitaxial films of  $\text{Bi}_2\text{Se}_3$ . The critical current temperature dependence is found in agreement with the Eilenberger theory, indicating ballistic transport and the existence of a global topological superconducting state induced in the TI film. If the number of flux quanta per unit cell,  $f$ , is an integer, the critical current showed a sharp local maximum. The effect is analogous to the Little-Parks effect: If  $f=n$  is an integer then each unit cell can accept  $n$  vortices, thus minimizing the circulating currents globally and reducing the energy to the level of the ground state at zero field. Unexpectedly, the expected critical current peak at  $f=2$  was missing in our arrays. Thus, at such field ( $f=2$ ) the usual  $2\pi$  invariance of the array Hamiltonian breaks down, although the array remains superconducting globally. Interestingly, the value of the critical current at  $f=2$  matches the estimated current carried by Majorana zero modes. We propose that such topological superconducting arrays can be used as sources of Majorana topological currents.

# RPPR Final Report

## as of 19-Apr-2021

**Training Opportunities:** Training is provided to the students participating in this project. It includes cryogenic experiments, high precision electrical measurements, sample design, electron beam lithography and other nanofabrication techniques, metal deposition, programming in experiment-related languages, such as LabView and Python, publishing research results, ethics of scientific research, oral presentations, and others.

**Results Dissemination:** The results on bulk-insulating topological insulator epitaxial films have been published in PHYSICAL REVIEW LETTERS 124, 236402 (2020).  
One more publication, related to the missing peak effect in the square array is now under preparation.

**Honors and Awards:** Nothing to Report

**Protocol Activity Status:**

**Technology Transfer:** Nothing to Report

### PARTICIPANTS:

**Participant Type:** PD/PI

**Participant:** Alexey Bezryadin

**Person Months Worked:** 1.00

Project Contribution:

National Academy Member: N

**Funding Support:**

**Participant Type:** Co PD/PI

**Participant:** James Eckstein

**Person Months Worked:** 1.00

Project Contribution:

National Academy Member: N

**Funding Support:**

**Participant Type:** Graduate Student (research assistant)

**Participant:** Xiangyu Song

**Person Months Worked:** 6.00

Project Contribution:

National Academy Member: N

**Funding Support:**

**Participant Type:** Graduate Student (research assistant)

**Participant:** Yang Bai

**Person Months Worked:** 6.00

Project Contribution:

National Academy Member: N

**Funding Support:**

**Participant Type:** Faculty

**Participant:** Dale Van Harlingen

**Person Months Worked:** 1.00

Project Contribution:

National Academy Member: N

**Funding Support:**



## **Final Report**

**Army W911NF-19-0067**

**Total budget \$150,000; ended 12/20/21**

**PI: Alexey Bezryadin (Physics, UIUC)**

**Co-Pi: James Eckstein (Physics, UIUC)**

## **Major Goals**

Topological superconductors are among the most unconventional states of matter, wherein exotic p-wavelike pairing and time-reversal symmetry can foster supersymmetry and zero-energy excitations called Majorana bound states. Although potential applications of theoretically proposed topologically protected quantum computers are numerous, the basic demonstration of non-Abelian behavior has not been achieved yet. Thus, our major goal is to design fabricate and test suitable electronic devices which can unambiguously demonstrate topological protection and non-Abelian behavior.

Among many obstacles, the materials issues are still of great importance: Many of the synthesized topological insulator materials exhibit bulk conductivity, while, in theory, only the surface is supposed to be conducting, while the bulk conductivity should be zero. Thus, an important goal of this project is to discover, develop, synthesize, and test novel topological systems approaching the ideal case in which the current is carried predominantly by the topological states. Another goal is to characterize these materials using available powerful techniques, providing access to the electronic spectrum structure, such as angle-resolved photoemission spectroscopy (ARPES).

As the material issues get improved, we target implementations of novel hybrid devices and structure involving the top-quality topological insulators interfaced with superconducting Nb films. In such systems, superconducting electrons penetrates into the topological insulator, due to the proximity effect. The induced superconductivity is expected to acquire topological properties of the host topological insulator.

The main plan is to fabricate multiterminal devices in which non-Abelian Majorana particles are predicted theoretically. The devices and systems should allow flexibility and control over the phase of the induced, complex-function, superconducting order parameter. The guiding principle is that the Majorana states are expected in the segments of Josephson junctions at which the phase difference equals  $\pi$ . If such condition is satisfied, the energy of the quasiparticles approaches zero, and, due to the underlying topological properties, the localized quasiparticles should become the desired non-Abelian Majorana states.

The key feature of the Majorana zero modes is that they have a ground state degeneracy characterized by the so-called "parity". This degeneracy, if discovered, can be used for storing and processing quantum information in a topologically protected manner. Yet, they parity has not been observed in any experiment yet. Another fundamental property of the Majorana zero modes is called braiding. The physical meaning of this property is that if two Majorana localized modes are moved around each other then the ground state should change its parity. This way one hopes to be able to process quantum information in the future topologically protected quantum computers. A long-term goal of this project is to design systems where such fundamental properties of the Majorana states could be demonstrated.

Practically, our approach is to focus on arrays with multiple electrodes and multiple superconducting islands, coupled to high quality epitaxial topological insulator films. In such systems phase differences of the complex superconducting order parameter can be controlled by applying external magnetic fields. Thus, it should be possible to induce Majorana zero modes, which are expected to occur in Josephson vortices. The parity effect should be detectable as fluctuations of the net supercurrent in the system or fluctuations of the critical current/kinetic inductance. Thus, the braiding phenomenon can probably be tested by moving vortices in and out the array, assuming that some vortices will experience an entanglement of their paths. Precise control of the vortex position can also be achieved if calibrated current pulses are applied. Such braiding events should cause parity changes and should be detectable in transport or the kinetic inductance measurements.

## **Accomplishments Under Goals:**

### **1. Proximity Pairing in Topological $(\text{Bi}_{1-x}\text{Sb}_x)_2\text{Te}_3$ Films on Niobium**

One major result of this project is the ultrahigh-resolution ARPES mappings of clean, bulk insulating  $(\text{Bi}_{1-x}\text{Sb}_x)_2\text{Te}_3$  ( $x \sim 0.62$ ) on superconducting Nb substrate as a function of TI film thickness and temperature. This material is extraordinary since it is an intrinsic topological insulator. The Fermi level in this material is tuned to the topological states and it avoids bulk conduction states. The results, combined with the previous studies of the  $\text{Bi}_2\text{Se}_3/\text{Nb}$  interface, reveal the pivotal role of bulk states in transitioning superconductivity to the surfaces of TIs-Nb hybrid systems [1].

This project is motivated by the following considerations. Topological superconductors are among the most unconventional states of matter, wherein exotic p-wavelike pairing and time-reversal symmetry can foster supersymmetry and zero-energy excitations called Majorana bound states. These emergent quasiparticles obey a non-Abelian statistics pertinent to topological quantum computing. Despite some recent progress, robust topological superconducting states remain elusive due to, often small, superconducting gap and low transition temperature in candidate materials. One promising alternative for realizing this state is to couple topological insulators (TIs) to a superconductor (SC) so that p-wave-like pairing is induced into the topological boundary states via the superconducting proximity effect. Thus, the proximity effect is at the focus of this project.

In this project the superconductor of choice, needed to introduce superconductivity in the hybrid systems, is Nb. To circumvent the inherent difficulties in growing TIs on Nb substrates, a novel cleavage-based flip-chip method is employed (Fig.1), which upon cleaving yields the intrinsic TI films of specific thicknesses, even in the ultrathin-film limit, on superconducting bulk Nb films.

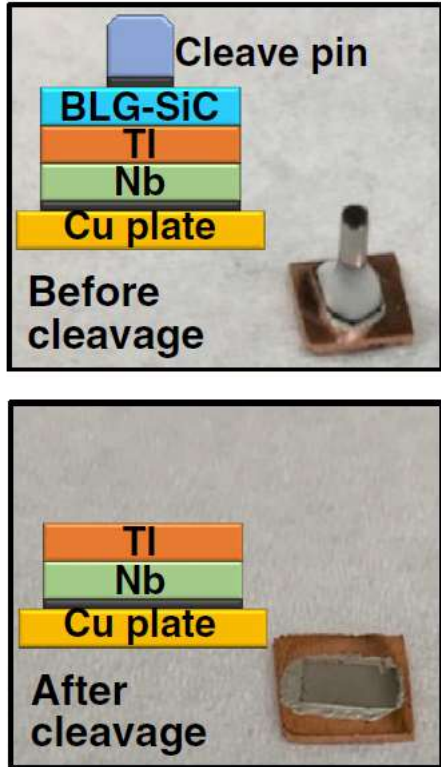


Figure 1. Photo and diagram of flip-chip sample structure before cleavage. (g) Similar as in (f) but after cleavage.

Proximity-induced superconducting gaps for slightly n-doped intrinsic topological insulator  $(\text{Bi}_{1-x}\text{Sb}_x)_2\text{Te}_3$  are quantified and contrasted with those of n-doped  $\text{Bi}_2\text{Se}_3/\text{Nb}$  from prior work conducted in the Eckstein group.<sup>2</sup> Proximity induced is observed and it is found that it is significantly stronger in the  $\text{Bi}_2\text{Se}_3/\text{Nb}$  system. But this system has a much larger concentration of bulk carriers. Thus, an important conclusion is reached that the bulk state, which are also made superconducting due to the proximity effect, play a key role in inducing superconductivity in the topological layer of the TI.

The series of square arrays and triangular arrays has been produced (Fig.2) and systematic measurements have been performed (Fig.3). Each array is a lattice of superconducting Nb islands placed onto a topological insulator film  $(\text{Bi}_{1-x}\text{Sb}_x)_2\text{Te}_3$ . The square arrays exhibit,

reproducibly, a global superconductivity below  $\sim 0.2\text{K}$  (Fig.2).

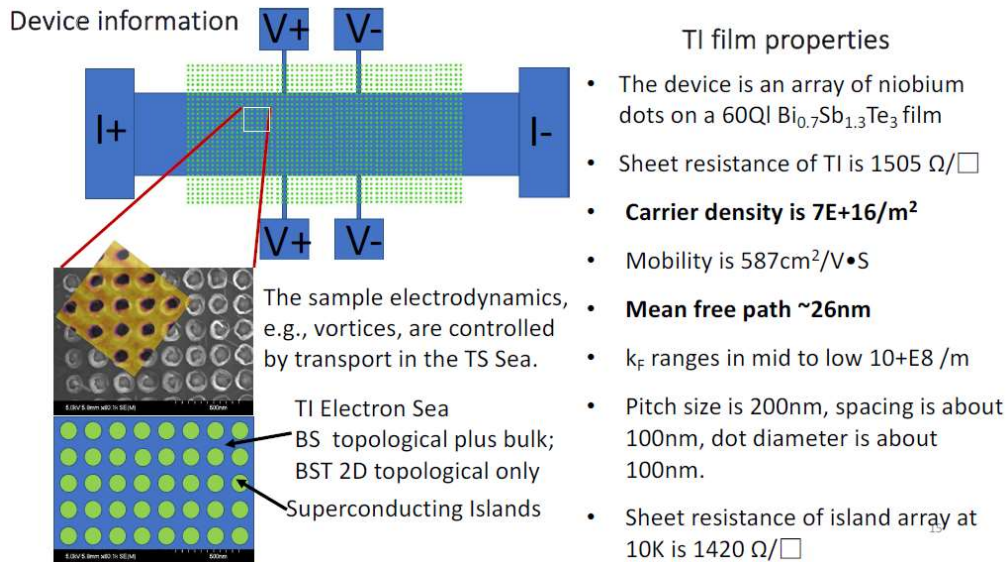


Fig.2. Results on the fabrication and testing of the topological arrays involving the intrinsic topological insulator.

Resistance vs Temp for similar arrays on BST and BS  
 different curves have different island spacings  
 Island diameter 100nm. Variable pitch

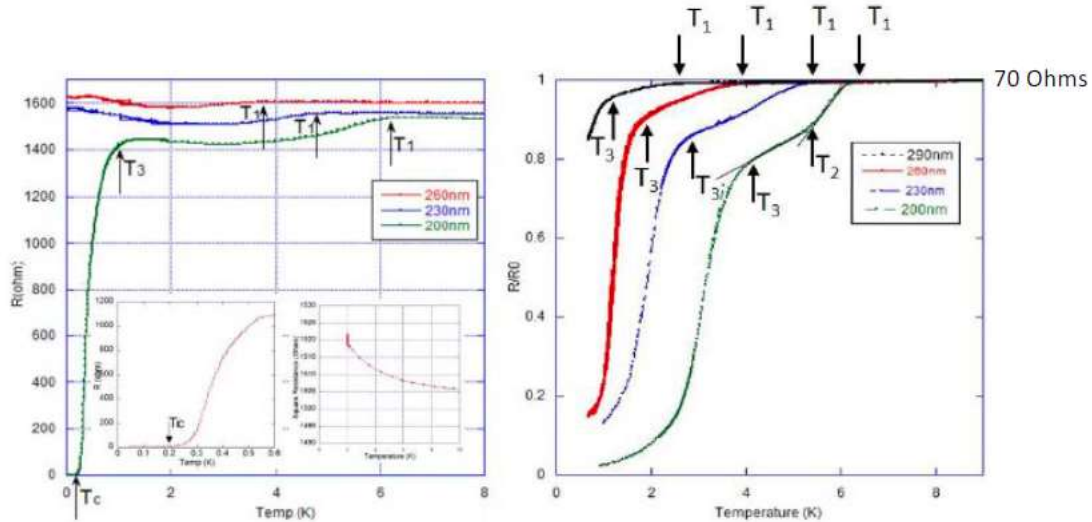


Figure 3. Result of the systematic study of the proximity-induced superconductivity in the intrinsic topological insulator system (left), as compared to non-intrinsic topological insulator sample (right).

## 2. Critical current and magnetic interference effects in topological superconducting arrays of Nb islands coupled through Bi<sub>2</sub>Se<sub>3</sub> epitaxial films

The proximity effect and the search for Majorana states has been conducted in superconducting arrays, as presented below. The studied Nb-Bi<sub>2</sub>Se<sub>3</sub>-Nb arrays consist of Nb square islands arranged into a square lattice (Fig.3). The Nb islands are placed onto an epitaxial, 60 nm thick, Bi<sub>2</sub>Se<sub>3</sub> film, as shown in Fig.3 (inserts). The lateral dimensions of niobium island are 1.2 $\mu$ m x 1.2 $\mu$ m and the thickness is 100 nm. The gap between neighboring islands is ~100-200 nm. The array is fabricated by electron beam lithography and plasma sputtering of Nb films and contains 23 x 23 Nb islands, which act as quasi-independent superconducting electrodes. These islands introduce a superconducting order parameter, of a certain amplitude and phase, in the underlying TI, by the proximity effect. Due to the proximity effect, the topological insulator becomes superconducting, including the regions in between the Nb islands. Thus, the entire array becomes globally superconducting if the temperature is sufficiently low.

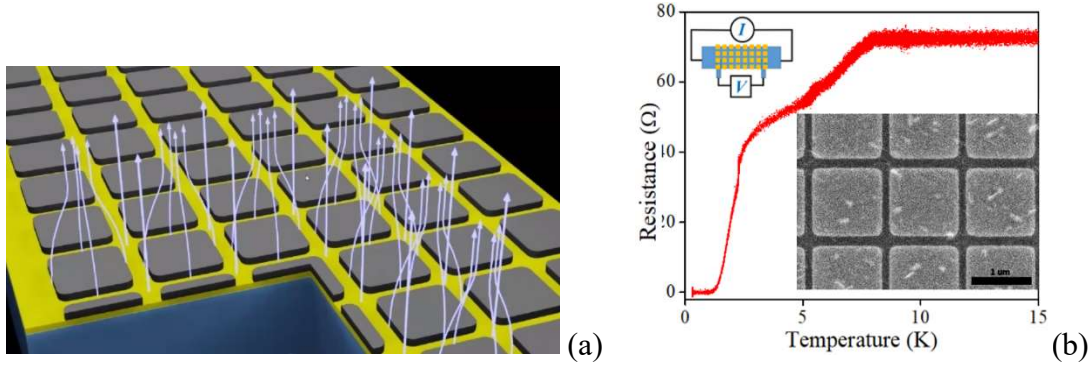


Fig.3 (a) Schematic of the sample: Nb square islands (grey) form a periodic square lattice (the array). The applied magnetic field penetrates mostly in the gaps between the islands. The Nb islands are placed over a topological insulator film (green). (b) Resistance versus temperature dependence for the array 3525-1. The top insert shows the schematic of the measurement circuit; the bottom insert is scanning electron microscope (SEM) image of a part of the array. The scale bar in black is  $1 \mu\text{m}$  long.

The resistance versus temperature dependence is shown in Fig.3. The resistance partial drop at 8 K is due to the superconducting transition of the Nb islands and the topological insulator regions located immediately below the islands. The second resistance drop (to zero), occurring at  $\sim 2$  K, signifies the establishment of global superconductivity involving the regions of the TI located between the islands. The voltage-current dependence, V-I curve, measured at 60 mK, is shown in Fig.4. The voltage is zero up to the critical current ( $I_c$ ), meaning that phase slip diffusion does not take place (at this low temperature) as long as the current is below the critical current.

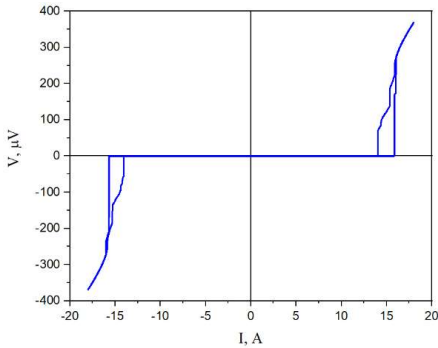


Fig.4 A representative V-I curve of the superconducting array 3525-1 measured at 60 mK and nominally zero magnetic field. The critical current is marked by a sharp jump of the voltage from zero to a finite value of the order of 10 to 100  $\mu\text{V}$ .

The critical current as a function of temperature is shown in Fig.5. At higher temperatures, the dependence shows a positive curvature, which is suggestive of a ballistic transport. We perform a detailed analysis of the proximity effect. The fit is calculated under the assumption of ballistic electron transport, using Eilenberger equation.

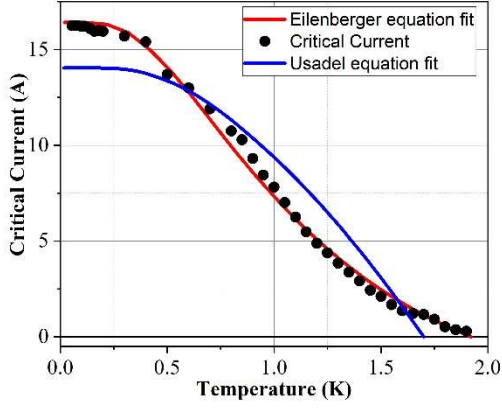


Figure 5. Critical current versus temperature. The black circles represent the data, and the red fit is generated according to the theory of ballistic Josephson junctions<sup>15</sup>. The blue fit is generated according to the theory of diffusive junctions. Sample 3525-1.

The ballistic theory predicts that the supercurrent,  $I_s$ , supported by  $N$  surface modes can be calculated as

$$I_s = N \frac{2\pi}{\hbar} e k_B T \sin\varphi \sum_{\omega_n > 0} \int_0^1 \mu d\mu \frac{t_1(\mu)t_2(\mu)}{\sqrt{Q(\varphi, \mu)}}$$

where  $\varphi$  is the phase difference between the superconducting electrodes,  $\mu = k_x/k_F$  is the integration variable,  $k_F$  is the Fermi wave vector,  $k_x$  is a wave vector of ballistic mode along the junction (i.e., in the direction of the current flow),  $N$  is the amount of conducting channels,  $t = \frac{D}{2-D}$ ,  $D$  being the transparency of each of the two S/N interfaces, and

$$Q = [t^2 \cos\varphi + (1 + (1 + t^2) \frac{\omega_n^2}{\Delta^2}) \cosh \frac{2\omega_n L}{\mu \hbar v_F} + 2t \frac{\omega_n \Omega_n}{\Delta^2} \sinh \frac{2\omega_n L}{\mu \hbar v_F}]^2 - (1 - t^2)^4 \frac{\Omega_n^4}{\Delta^4},$$

where  $L$  is a junction length,  $\omega_n$  is Matsubara frequency. The coherence length is defined as  $\xi_0 = \hbar v_F / \pi k_B T_c$ ,  $\Omega_n = \sqrt{\omega_n^2 + \Delta^2 \cos^2(\frac{\varphi}{2})}$ , and  $\Delta$  is the gap induced into topological insulator crystal. The effective critical temperature,  $T_c$ , is defined formally through the BCS equality  $\Delta = 1.76 k_B T_c$ , where  $\Delta$  is a fitting parameter representing the energy gap induced in Bi2Se3 through the proximity effect of Nb islands. Here  $k_B$  is the Boltzmann constant. The induced gap is assumed to depend on temperature according to the Bardeen-Cooper-Schrieffer (BCS) theory.

For the ballistic theoretical model (red) used in generating the fit in Fig.5 the following parameters have been used: the effective critical temperature  $T_c = 1.82$  K, the Fermi velocity  $v_F = 2.8 \times 10^5$  m/s,<sup>2</sup> the length of the junction in the direction of the current flow  $L = 206$  nm, the number of ballistic channels in the entire array, contributing to the supercurrent,  $N = 1090$ . This corresponds to  $N_1 = 47$  channels per junction.

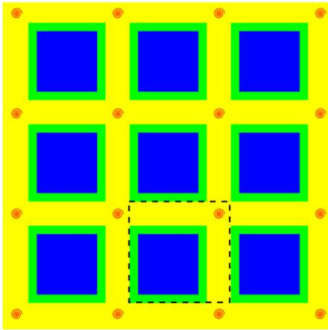
The agreement with the theory is excellent (Fig.5). The theory captures the most prominent qualitative features of the measured curve  $I_c(T)$ , namely that the curvature of the  $I_c(T)$  function is

positive at higher temperatures and it becomes negative at lower temperatures. The inflection point occurs roughly at the temperature which is twice lower than the critical temperature.

The fit calculated under the assumption of diffusive electronic transport has been tested also (Fig.5). The model differs from the data qualitatively since it predicts negative curvature in the entire temperature interval, while the data show a clear positive curvature at higher temperatures.

The results presented above indicate that the transport in the array is ballistic. Thus, a *global topological superconducting state* can be conjectured in the topological insulator film. Non-topological states could not provide ballistic transport since the mean free path is not sufficiently long in the bulk. Vortices induced by an external magnetic field in such superconductors have been predicted to sustain Majorana zero modes. Below we present transport measurements in perpendicular magnetic fields.

To quantify the applied perpendicular magnetic field, we express it in terms of the normalized flux per unit cell,  $f = \Phi / \Phi_0$ , where  $\Phi = a^2 B$  is the flux per unit cell,  $a$  is the distance between the Nb island centers (the size of the unit cell),  $B$  is the applied field and  $\Phi_0 = 2.06 \times 10^{-15} \text{Wb}$  is the flux quantum. The unit cell is a square, as is shown by a dashed line in Fig.4. The unit cell width equals the island width plus the width of the gap between neighbor



islands. Each unit cell has two junctions, one horizontal and vertical junction, corresponding to rectangular yellow regions inside the dashed line square of Fig.6.

*Fig.6 A segment of the Nb-on-TI array is shown schematically. The magnetic field in this example satisfies the first matching condition,  $f=1$ , i.e., there is one vortex per unit cell. The vortex is shown schematically, as a single swirl present in each unit cell and located between the corners of the squares. Blue: flux-free area, i.e., the Meissner state of the superconducting Nb islands. Green: flux penetrating at the edges of the Nb islands. Yellow: topological insulator film, where superconductivity is induced due to the proximity effect. The black dashed line shows the square unit cell of the lattice having periodicity  $a=1.2 \mu\text{m}$ .*

When a magnetic field is applied perpendicular to the unit cell, most of the field lines concentrate between the superconducting islands, due to the Meissner effect (Fig.3a, Fig.6). The field was always sufficiently weak so that vortices do not enter into the Nb islands. The number of induced vortices per unit cell is given by the normalized flux,  $f$ , defined above. So, if  $f=1$ , there is exactly one vortex in the unit cell. The most favorable arrangement is the square lattice of vortices shown in Fig.6. The vortices, schematically shown as swirls, represent points such that the phase winds by  $2\pi$  on a closed path going around such points. Such vortex lattice, due to its perfect commensurability with the lattice of Nb islands, experiences the strongest pinning; also, this state represents the lowest energy of the system, which, in the limit of small islands, equals

the energy at zero field. Thus, the critical current is expected to show a sharp maximum at  $f=1$ . The measurement of the array resistance as a function of the perpendicular magnetic field confirms such expectations: The resistance exhibits a sharp minimum at  $f=1$  (Fig.7).

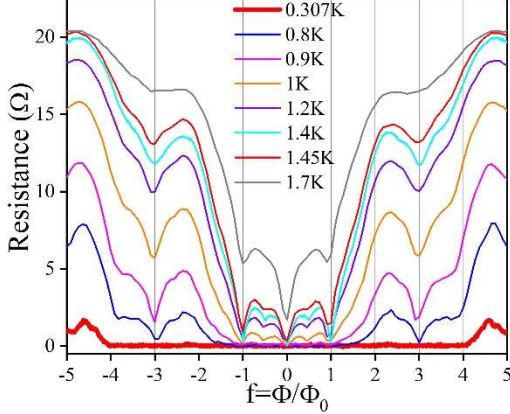


*Fig.7 Sample 3525-1. Resistance versus magnetic flux per unit cell, normalized by the flux quantum. The red curve is measured at  $T=307$  mK and a bias current of  $\sim I_c/10$ .*

Magnetic field sweep (Fig.7) shows the device resistance oscillates as the flux per unit cell,  $f$ , is increased. In particular, another pronounced sharp drop of the resistance (and the corresponding sharp increase of the critical current) is observed at  $f=3$ , at which there are three vortices per unit cell. Such resistance minima at  $f=1$  and  $f=3$  are expected based on the argument that at integer values of  $f$  the induced vortex lattice is commensurate with the lattice of Nb islands and thus should be well pinned. This same condition corresponds to the energy minimization principle. So, the motion of vortices by the Lorentz force, and/or due to thermal fluctuations, is suppressed by the periodic pinning potential. Thus, the vortices move less and, correspondingly, the voltage and the resistance are strongly reduced.

In previous studies of non-topological arrays, the sharp resistance minima and CC maxima have been observed at all integer values of the normalized flux,  $f$ , including  $f=2$ . An unexpected result of our experiments on the topological superconducting arrays is that the peak corresponding to  $f=2$  is absent.

Different competing structures of the vortex lattice are possible at the magnetic field bias  $f=2$ ; they are illustrated in Fig.8. In the first case (Fig.8a) all the Josephson vortex centers accumulate at the points of the lowest induced superconducting gap, namely in the space between the four corners of the neighbor Nb squares. In such scenario the pinning of the vortex lattice should be strong at  $f=2$ , so the critical current should exhibit a strong maximum. The experiment clearly shows that this is not the case, so we conclude that the arrangement of Fig.6a is not realized in our arrays at  $f=2$ . Yet, based on the result of Fig.8, we conclude that the pinning amplification due to the commensurability effect does happen while at  $f=1$  and  $f=3$ , i.e., at these values of the frustration coefficient the energy has a deep local minimum, and, correspondingly, the critical current exhibits a pronounced maximum.

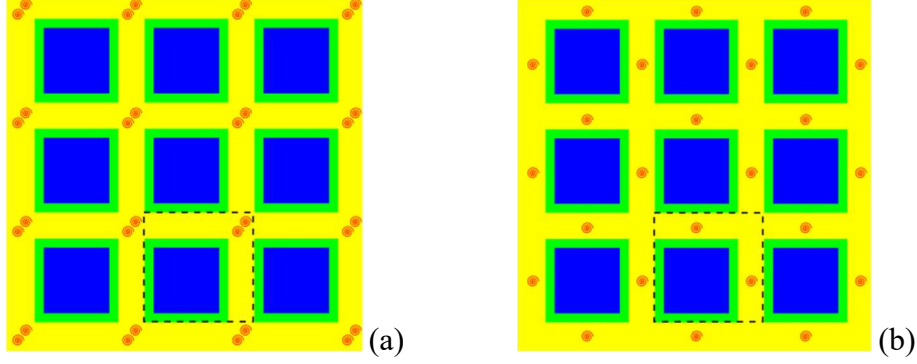


Fig.8. Possible arrangement of the vortex centers (vortex cores), for the normalized flux  $f=2$ . The number of vortices per unit cell equals two in all cases. (a) Two vertices in each unit cell occupy the point of the lowest superconducting gap, namely the space between the four corners of the neighbor squares. (b) In the second scenario, the centers of the vortices are located inside (in the middle) of the Josephson junctions, thus suppressing the pair supercurrent due to the Fraunhofer effect.

Another possible scenario for the vortex arrangement, at  $f=2$ , is shown in Fig.8b. Since each unit cell of the array contains two junctions, the  $f=2$  condition translates, at least approximately, into the condition that each junction contains one vortex, because there is one quantum of the applied magnetic flux in it. In the Fig.8b scenario, the suppression of the critical current occurs due to the Fraunhofer-type interference, since the supercurrent changes its sign within each junction, so the integral over the entire width of the junction is zero. Yet, the experiment shows that the critical current is not zero at  $f=2$ . This apparent disagreement with Fig.8b model is the key result of this experiment.

To further elucidate the anomalous behavior at  $f=2$  we have measured another sample 3525-2. This sample is very similar to 3525-1, except that the critical current is slightly lower since the distance between the edges of neighbor Nb islands was slightly larger. (This distance is referred to as the length of the junction,  $L$ .) The results (Fig.9) are presented in a form of a three-dimensional (3D) color-coded plot of the differential resistance  $dV/dI$ . There, the x-axis is the magnetic field, and the y-axis is the bias current. The blue region is the region where the voltage is zero, so that the border of the blue region represents the critical current.

The Fig.9 leads to the following conclusions: (i) There is no local maximum of the critical current at  $f=2$ , while the maxima are clearly visible at  $f=0, 1, \text{ and } 3$ . (ii) Broad critical current minima are observed at fields  $H_f, 2H_f, 3H_f, \text{ etc.}$ , which represent the condition of integer of flux quanta per junction. (iii) The condition  $f=2$  occurs at a somewhat weaker field than the condition  $H=H_f$ . (iii) The critical current does not go to zero neither at  $f=2$  nor at  $H=H_f$ . Thus, the magnetic Fraunhofer interference effect is not able to fully suppress superconductivity and bring the critical current to zero, as would be expected for in ideal non-topological junction.

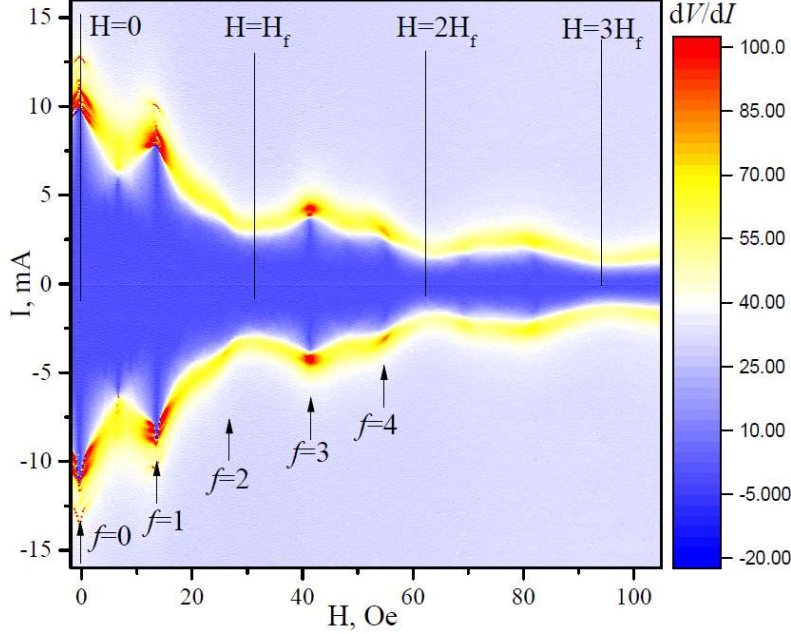


Figure 9. Differential resistance,  $dV/dI$ , measured in Ohms, is plotted using the color-coding shown on the right side. The  $dV/dI$  is plotted versus the magnetic field (the horizontal axis) and the bias current (the vertical axis). The vertical black lines are periodically positioned with the period being  $H_F$ , representing the Fraunhofer effect, i.e., integer numbers of the flux quantum penetrating each Josephson junction. The vertical arrows represent the normalized flux per unit cell of the array.  $T=60$  mK.

For the square array considered, the flux per unit cell,  $\Phi_{\text{cell}}$  is about twice larger than the flux per junction,  $\Phi_j$ , due to the geometry. Thus, there is a special value of flux of a particular interest, namely the case when the flux per unit cell equals two flux quanta,  $\Phi_{\text{cell}}=2\Phi_0$ . At such value of the external field  $\Phi_j=\Phi_0$ , and thus the Josephson supercurrent between the Nb islands should be supposed to be zero, irrespective of the phase difference between the Nb islands. Such observation would explain why the expected maximum of the critical current is missing at  $f=2$ . This explanation appears to break down since a non-zero supercurrent is measured at  $\Phi_{\text{cell}}=2\Phi_0$ , as well as at  $H=H_F$ .

To the best of our knowledge there is no fully developed theory of topological arrays which would be able to predict the arrangement of vortices at integer values of the flux and the corresponding critical current of the array. Below we propose an estimate to the effect observed.

The facts that the supercurrent does not go to zero at  $f=2$  provides evidence that the Majorana zero mode (MZM) current, which is expected to occur between the MZMs localized at the cores of the vortices, contributes significantly to the measured total supercurrent. To confirm this possibility, we estimate the net supercurrent contributed by the hypothetical MZM. If each vortex contains one MZM and a pair of MZM is needed to sustain a supercurrent, as was argued

in the theory, then the total supercurrent will be equal to the supercurrent associated with one conduction mode multiplied by the number of islands,  $N_w$ , in a horizontal row of the lattice (here  $N_w=23$ ). The estimate of the Majorana contribution to the supercurrent, as  $I_M=\Delta/\Phi_0$ . According to a direct measurement of the energy gap in Nb-on-Bi2Se3 bilayer systems the induced gap in the surface layers of the TI is  $\Delta\sim 1$  meV. So, the Majorana current per a pair of vortices is  $I_{M2}=\Delta/\Phi_0=77$  nA. This is the contribution of just one cell of the array, since each cell contains two vortices. The total MZM contribution is the number of cells across the array times the contribution from one cell of the array, i.e.,  $I_{M,tot}=N_w I_{M2}=1.8$   $\mu$ A. This is in a reasonable agreement with the experimentally observed value of the critical current at  $f=0$ , which is  $\sim 2.5$   $\mu$ A (Fig.9). Thus, the array can be used as a medium for Majorana current generation. The work is currently under preparation for publication.

### **Training Opportunities**

Training is provided to the students participating in this project. It includes cryogenic experiments, high precision electrical measurements, sample design, electron beam lithography and other nanofabrication techniques, metal deposition, programming in experiment-related languages, such LabView and Python, publishing research results, ethics of scientific research, oral presentations, and others.

### **Results Dissemination**

The results on bulk-insulating topological insulator epitaxial films have been published in PHYSICAL REVIEW LETTERS 124, 236402 (2020). The results on topological arrays are being prepared for publication.

### **References**

---

<sup>1</sup> J. A. Hlevyack et al., Physical Review Letters 124, 236402 (2020).

<sup>2</sup> Flötotto, David, et al. "Superconducting pairing of topological surface states in bismuth selenide films on niobium." Science advances 4.4 (2018): eaar7214.